

Published in final edited form as:

Stem Cells. 2013 October ; 31(10): . doi:10.1002/stem.1481.

Transplantation of human umbilical mesenchymal stem cells cures the corneal defects of Mucopolysaccharidosis VII mice

Vivien Jane Coulson- Thomas^a, Bruce Caterson^b, and Winston W-Y Kao^a

^aDepartment of Ophthalmology, College of Medicine, Edith J. Crawley Vision Research Center, University of Cincinnati, Cincinnati, OH 45267, USA

^bConnective Tissue Biology Laboratories, School of Biosciences, Cardiff University, Cardiff CF10 3AX, UK

Abstract

Mucopolysaccharidosis (MPS) are a family of related disorders caused by a mutation in one of the lysosomal exoglycosidases which leads to the accumulation of glycosaminoglycans (GAGs). MPS VII, caused by a mutation in α -glucuronidase, manifests hepatomegaly, skeletal dysplasia, short stature, corneal clouding and developmental delay. Current treatment regimens for MPS are not effective for treating corneal clouding and impaired mental development. We hypothesized that human umbilical mesenchymal stem cells (UMSC) transplanted into the corneal stroma could participate in the catabolism of GAGs providing a means of cell therapy for MPS. For such treatment, human UMSC were intrastromally transplanted into corneas of MPS VII mice. UMSC transplantation restored the dendritic and hexagonal morphology of host keratocytes and endothelial cells, respectively, and *in vivo* confocal microscopy (HRTII) revealed reduced corneal haze. Immunohistochemistry using antibodies against HS and CS chains as well as LAMP2 revealed a decrease in GAG content and both lysosomal number and size in the treated corneas. Labeling UMSC intracellular compartments prior to transplantation revealed the distribution of UMSC vesicles throughout the corneal stroma and endothelium. An *in vitro* co-culture assay between skin fibroblasts isolated from MPSVII mice and UMSC demonstrated that neutral vesicles released by the UMSC are taken up by the fibroblasts and proceed to fuse with the acidic lysosomes. Therefore, transplanted UMSC participate both in extracellular GAG turnover and enable host keratocytes to catabolize accumulated GAG products, suggesting that UMSC could be a novel alternative for treating corneal defects associated with MPS and other congenital metabolic disorders.

Keywords

Mucopolysaccharidosis; umbilical cord mesenchymal stem cells; cornea; glycosaminoglycans; exosomes

Correspondence: Vivien Jane Coulson- Thomas PhD or Winston Kao PhD, Department of Ophthalmology, University of Cincinnati, CARE/Crawley Bldg. RM 5860, 3230 Eden Avenue, Cincinnati, OH 45267-0838 vivien.coulson-thomas@uc.edu or kaoww@ucmail.uc.edu.

Author Contributions: V.J.C-T: conception and design, collection and assembly of data, data analysis and interpretation, manuscript writing and final approval of the manuscript; B.C. supplied reagents, final approval of the manuscript; W.W.-Y.K.: conception and design, data analysis and interpretation and final approval of the manuscript.

Disclosure of Potential conflicts of interest

The authors indicate no conflict of interest.

Introduction

Mucopolysaccharidosis (MPS) are a family of related disorders caused by a mutation in one of the lysosomal exoglycosidases required for the sequential degradation of glycosaminoglycans (GAGs), which leads to their multi-organ lysosomal storage^{1, 2}. GAGs, previously referred to as mucopolysaccharides, are long unbranched polysaccharides consisting of repeating disaccharide units composed of a hexosamine (glucosamine or galactosamine) and a hexuronic acid (glucuronic or iduronic acid) generating heparan sulfate (HS), heparin (HEP), chondroitin sulfate (CS) and dermatan sulfate (DS). To date eleven different enzymatic defects have been characterized leading to seven types of MPS. MPS are chronic and progressive diseases with a high prevalence of morbidity, including skeletal and joint abnormalities, hepatomegaly and splenomegaly, cardiovascular and respiratory dysfunction, neurological dysfunction, hearing and vision loss, and short life expectancy^{3, 4}. Clinical manifestations vary among the specific MPS classes and also according to the genetic background in which the patient may carry a mutation with residual enzymatic activity^{5, 6}. Moreover, as the disease progresses the accumulation of metabolic derivatives in the lysosomes compromises cell functions and ultimately leads to cell death, which consequently leads to further accumulation of GAG-derivatives in the extracellular matrix (ECM), blood and urine. MPS VII, also known as Sly syndrome, is caused by a mutation of α -glucuronidase which leads to the accumulation of HS (HEP), DS and chondroitin-4- and -6-sulfate⁷⁻⁹. Clinical manifestations of MPS VII are hepatomegaly, skeletal dysplasia, short stature, corneal clouding and delayed development^{3, 10-12}. In the more severe cases of MPS VII, patients are stillborn or survive a few months after birth, however, most MPS VII patients live into teenage or young adult years. Patients who suffer a milder form of MPS VII, due to a mutation which translates to an enzyme with residual activity, may survive into adulthood, with some patients reported to live into the fifth decade⁵. The incidence of each MPS varies greatly according to region and race and, therefore, incidence estimates for the various types of MPS show considerable variation; however the incidence of an MPS is approximately 1 in 46,000 births¹³.

Current treatment for MPS is enzyme replacement therapy and/or bone marrow transplant; however, these forms of therapy are not effective for ameliorating the corneal clouding and impaired mental development due to corneal avascularity and the blood/brain barrier, respectively¹⁴⁻²⁵. Therefore, new forms of treatment must be explored for corneal defects in MPS VII patients. Currently, keratoplasty is the only option for treating corneal clouding of MPS, which is not possible in more advanced cases in which patients are too frail to undergo anesthesia. Moreover, due to the shortage of transplantable corneas as well as the complications entailed by corneal transplantation, alternative treatments are required for the prevention and cure of corneal blindness in lieu of corneal transplantation. Umbilical mesenchymal stem cell (UMSC) transplantation has been shown to successfully recover the transparency and increased corneal thickness of lumican null mice ($Lum^{-/-}$)²⁶. Interestingly, these cells assume a keratocyte phenotype and present collagen lamellae re-organization²⁶. Thus, we hypothesize that human UMSC intrastromally transplanted into MPS mice will assume a keratocyte phenotype and catabolize accumulated extracellular GAGs restoring corneal functions. In the cornea, CS and DSPGs, such as biglycan and decorin, are essential structural components of the stroma, where they regulate the collagen fibril organization necessary for corneal transparency²⁷⁻²⁹. HSPGs, such as perlecan and syndecan- 1, form the basement membrane zone and are vital for keratocyte and epithelial cells function^{30, 31}. In order to treat the corneal phenotype associated with MPS VII human UMSC isolated from neonatal umbilical cords were intrastromally transplanted into corneas of 1, 2 and 3 month-old MPS VII mice. *In vivo* confocal microscopy of MPS mouse corneas at 3.5 months revealed that the stromal keratocytes display an amoeboid shape as well as significant corneal haze. In contrast, corneas treated with UMSCs at 1, 2 and 3 months presented

keratocytes with a dendritic cell shape and reduced corneal haze. Corneas treated at 1 or 2 months presented significantly improved corneal integrity when compared to mice treated at 3 months suggesting that prophylactic treatment upon diagnosis could prevent the development of corneal clouding. An overall decrease in GAG content was detected in corneas treated at all timeframes when compared to that of untreated MPS VII corneas. Interestingly, intercellular trafficking of vesicles was shown to occur between donor UMSC and recipient keratocytes. Therefore, corneal transplantation of UMSC is a potentially novel alternative for treating corneal defects associated with congenital metabolic disorders.

Material and Methods

Experimental mice

B6.C-H2-Kbm1/ByBir-Gusbmps/BrkJ breeding pair was obtained from The Jackson Laboratory (Bar Harbor, ME). B6.C-H2-Kbm1/ByBir-Gusbmps/BrkJ carry a point mutation mapped to the beta-glucuronidase gene complex on the distal end of chromosome 5 generating a mouse model for MPS VII. Genotyping was performed by digesting the PCR product generated using the following set of primers: forward CCTGTCTCATTTCATGTG and reverse GATAACATCCACGTACCGG, with the restriction enzyme NciI. Littermates not carrying the mutant allele as well as heterozygous mice were used as Controls and both yielded equivalent results. Animal care and use conformed to the ARVO Statement for the Use of Animals in Ophthalmic and Vision Research. All animal protocols were approved by the Institutional Animal Care and Use Committee (IACUC) of the University of Cincinnati.

Cell culture

Umbilical cords were obtained from the Christ Hospital according to protocols approved by the Institutional Review Board (IRB) of the University of Cincinnati Medical Center. Upon arrival umbilical cords were washed with 70% ethanol and subsequently excess blood was removed with sequential washes in EBSS. Blood vessels were removed, tissue minced into fine pieces and incubated with 0.05% trypsin (Gibco, CA) and 300U collagenase (Stem Cell Technologies) in alpha-MEM (Gibco) for 4 hours at 37°C. Thereafter, the cell suspension was filtered, centrifuged at 400×g and the cells cultured in alpha-MEM supplemented with 10% fetal bovine serum (FBS-Hyclone, MA) in 5% CO₂ atmosphere at 37°C. After 16 hours, the medium was changed to remove non-adherent cells. Thereafter, the medium was changed every 2 to 3 days and cells harvested at approximately 70% confluency with Trypsin/EDTA and subsequently seeded at a density of 3–6 × 10³ cells/cm². Cells at the fourth passage were stored in liquid N₂ as previously described²⁶.

Treatment of MPS VII mice with stem cells

MPS VII mice were treated with UMSC at three different time frames. One-month old animals were treated and corneas analyzed at 3.5 months of age, therefore, the stem cells were in the cornea for 10 weeks, 2 animals were treated at this time frame. Two-month old animals were treated and corneas analyzed at 3.5 months of age, therefore, the stem cells were in the cornea for 6 weeks, 12 animals were treated at this time frame. Three-month old animals were treated and corneas analyzed at 3.5 months of age, in which case the stem cells were in the cornea for 2 weeks, 6 animals were treated at this time frame (Fig. S1).

Intrastromal injection

Intrastromal injection was performed by first creating a small tunnel through the corneal epithelium into the anterior stroma using a 32-gauge needle with a sharp tip (Hamilton Co., NV). Thereafter, a blunt 33-gauge needle attached to a 10 µl Hamilton syringe (Hamilton

Co.) was passed through the tunnel into the corneal stroma and 2 μ l containing 10^4 cells were injected into the stroma. The cells were pre-labeled with DiI for 15 minutes at 4°C and subsequently washed 3 times with EBSS prior to intrastromal administration, enabling visualization of the cells within the stroma. DiI is a long-chain dialkylcarbocyanine that fluoresces when incorporated into the plasma membrane. DiI is transferred from labeled to unlabeled cells solely by DiI labeled membrane transfer and not by diffusion.

In vivo confocal microscopy

Analysis of stromal haze was performed with Heidelberg Retinal Tomograph-HRTII Rostock Cornea Module (HRT-II, Heidelberg Engineering Inc., Germany) according to the manufacturer's instructions. Briefly, GenTeal® Gel (Novartis Pharmaceuticals Corp., New Jersey) was applied to both the eyeball and the tip of the HRT-II objective as immersion fluid. Subsequently, a series of 40 images were collected to cover the whole stromal thickness as a continuous z-axis scan through the entire corneal stroma at 2 μ m increments starting from the basal layer of the corneal epithelium and ending at the corneal endothelium (the lens of HRT-II has a working distance of 77 μ m). A representative image at a stromal depth of approximately 8 μ m is displayed in Figure 2 and every fourth plane is presented in Fig. S2. In vivo confocal microscopy was also utilized to analyze stromal morphology and the integrity of the keratocytes. Keratocytes classically have a dendritic (fibroblast-like) cell shape which was determined by the presence of large, flat elongated (fusiform and/or spindle shaped) cells with branched cytoplasmic projections and amoeboid cells were determined as spherical cells with an irregular cell shape and size and loss of fibroblast-like morphology.

Confocal Microscopy and Whole mount

Eyeballs were excised and fixed for 30 minutes in 4% paraformaldehyde in phosphate buffered saline, pH 7.4 (PBS). After extensive washes in PBS the cornea button was removed and subsequently four small peripheral incisions were made in the cornea in order to enable posterior flat mount on a slide. Corneas were treated for 30 minutes with 0.2% sodium borohydride and thereafter extensively washed in PBS containing 0.2% Tween-20. Corneas were blocked overnight in 4% BSA in PBS containing 0.01 M saponin. Corneas were incubated overnight with rat anti-LAMP2 (Abcam, ab13524) or rat anti-ZO-1 (Millipore, MABT11) prepared in block solution at 4°C and subsequently washed in PBS and further incubated with secondary antibody or phalloidin (Invitrogen) in block solution for 8 hours at room temperature. Corneas were finally incubated with DAPI and mounted in Fluoromount G (SouthernBiotech).

Alcian blue staining

Sections were stained for 30 minutes in Alcian Blue solution (1% Alcian blue, 3% acetic acid) followed by three 1 minute washes with double distilled water. The nucleus was counter-stained with 0.1% Nuclear Fast Red Solution (0.1% Nuclear fast red, 5% aluminum sulfate).

Immunohistochemistry

Tissue sections (4 μ m) were incubated for 30 minutes at 37°C and subsequently washed 3 times in PBS. Tissue sections were incubated for 1 minute in 0.1 M glycine and subsequently incubated for 1 hour in blocking solution (5% FBS) at room temperature, and were then incubated with primary antibodies overnight at 4°C. Primary antibodies used were: mouse monoclonal anti-CS native sulfation motif epitope (clones 4C3 and 6C3) and anti-HS (10E4 epitope - US Biological). Afterwards, the tissues were washed 3 times in PBS and then incubated for 1 hour at room temperature with appropriate fluorescent secondary

antibodies produced in Donkey conjugated to Alexa Fluor[®] 488 or Alexa Fluor[®] 647 (Molecular Probes/Invitrogen, OR). After incubation with the antibodies, the cover slips were placed over the tissues with Fluoromount G (2:1 in PBS, Electron Microscopy Sciences, PA) and sealed with nail polish. Tissue sections were examined using a Zeiss Observer Z1 inverted microscope and images analyzed using LSM Image Browser 3.2 software (Zeiss, Germany).

Dimethylmethylene Blue assay

Two MPS VII animals were treated at 3 months and corneas collected after 2 weeks, 3 animals were treated at 2 months and corneas collected after 6 weeks, and 3 animals were treated at 1 month and corneas collected after 6 weeks. Total GAGs were extracted from each cornea by vigorously mincing the tissue with the use of surgical scissors in 50 μ L of 4M guanidinium chloride, 0.05 M sodium acetate, pH 6, and subsequently incubating the cornea overnight at 4°C. The buffer of the extract was changed to PBS with the use of Amicon Ultra 0.5 mL 3K Ultracel[®] (Millipore). The tissue was then digested with proteinase K for 24 hours at 60°C and subsequently incubated at 95°C for 30 minutes. Thereafter, total GAG content was assayed using the Dimethylmethylene Blue (DMB) assay. In short, 200 μ L of DMB reagent was added to 20 μ L of sample or standard, mixed and the absorbance immediately measured at 525 nm³². The total GAG content in the samples was calculated using a standard curve prepared with chondroitin 4-sulfate (Sigma). The GAG content of treated corneas (OD) was compared to that of littermate wild-type mice.

Second harmonic generation (SHG)

Whole-mount corneas were stained with SYTO[®] 59 (Life Technologies) and subsequently mounted in Fluoromount G. SHG was performed using a Zeiss Axiovert 200 inverted microscope platform with a 40x water immersion objective lens (numerical aperture, 1.2). SYTO[®] 59 images were obtained using 633 nm laser lines from the red He-Ne lasers. Emitted light was detected using 650 LP filters for SYTO[®] 59. Non-linear optical imaging of second harmonic generated signals (SHG) of collagen organization was performed using mode-locked titanium (MaiTai; Spectra-Physics Lasers Division, CA). The SHG forward-scattered signals were collected using a 0.8 NA condenser lens with a narrow band-pass filter (400/50) placed in front of the transmission light detector. Backward scattered SHG signals were detected with the Meta detector on the Zeiss LSM510 confocal microscope.

Cell-cell trafficking from UMSC to host keratocytes

UMSC were labeled with FM 1-43FX (Life technologies) for 30 minutes at 4°C and subsequently washed 6 times with EBSS prior to intrastromal transplantation. Eyeballs were excised after 3 days and corneas processed for whole mount.

Cell-cell trafficking from UMSC to fibroblasts isolated from MPS VII

A primary culture of fibroblasts was isolated from the skin of MPS VII mice, seeded on cover slips and maintained in alpha MEM medium supplemented with 10% bovine serum. UMSC were seeded in transwell inserts with 0.44 μ m pores (Millipore) or cover slips and left to adhere for 6 hours. UMSC were labeled with LysoSensor[™] Yellow/Blue DND-160 (Life Technologies) for 30 minutes. The nuclei of the UMSC and fibroblasts were labeled with SYTO[®] 59. Subsequently, the UMSC in the transwell inserts and on the coverslips were washed six times in HBSS. The transwell inserts containing UMSC were placed in the culture wells containing fibroblasts and left for 15, 30 or 60 minutes. UMSC and fibroblasts not placed in co-culture served as Controls. The live cells were analyzed using a Zeiss LSM710 confocal microscope.

Fibroblasts isolated from the skin of MPS VII mice were seeded on cover slips and UMSC were seeded in transwell inserts with 0.44 μm pores (Millipore). The cells were left to adhere for 6 hours and, subsequently, the transwell inserts containing UMSC were placed in culture wells containing fibroblasts and left for 6 hours. The fibroblasts were fixed and stained with LAMP2 as described above. The mean pixel intensity for LAMP2 staining was measured for twelve independent images captured for fibroblasts and for fibroblasts exposed to UMSC, and the averages displayed in a graph.

Statistics

All values are presented as means \pm standard deviation of the mean. The difference between two groups was compared by unpaired Mann-Whitney test. $P < 0.05$ was considered to be statistically significant. Statistical analysis was performed with the GraphPad Prism version 5 software package (GraphPad Software, San Diego, CA).

Results

Intrastromal transplantation of UMSC

UMSC previously labeled with DiI were transplanted into the right corneal stromas (OD) of 1, 2 or 3 month-old MPS VII mice (Fig. S3 A, C and E) and successful transplantation verified with the use of a 555 filter using a fluorescent stereo microscope. Left eyes (OS) served as contralateral controls. A significant number of UMSC delivered to the cornea were able to survive transplantation and persist in the corneas throughout the treatment period (Left panel in Fig. S3B, D and F).

In vivo confocal microscopy for the analysis of corneal integrity and haze

In order to evaluate the morphological changes of host cells upon UMSC transplantation *in vivo* confocal microscopy analysis of corneal integrity and stromal haze was performed. The corneas of MPS VII mice were examined at 3.5 months prior to the eyeballs being collected. *In vivo* confocal microscopy of untreated corneas (OS) from MPS VII mice revealed that MPS VII stromal keratocytes display an amoeboid shape as well as significant corneal haze (Fig. 1, Fig. 2 and Fig. S2). Both animals treated at 1 month of age presented dendritic shaped cells throughout the stroma, with no amoeboid keratocytes and no corneal haze (Fig. 1A and Fig. 2C). Animals treated at 2 months of age presented dendritic shaped cells throughout the stroma, with solely a few amoeboid keratocytes in the posterior stroma adjacent to the endothelium (Fig. 1B, Fig. 2D and Fig. S2). Moreover, a drastic decrease in corneal haze was observed for corneas from mice treated at 2 months of age compared to the untreated corneas (Fig. 1B). All 12 animals treated at this timeframe presented a significant improvement in stromal and keratocyte morphology. Corneas from mice treated with UMSC at 3 months of age presented a drastic decrease in keratocytes with an amoeboid shape and a significant decrease in corneal haze (Fig. 1C, Fig. 2F and Fig. S2). Moreover, an improvement in keratocyte morphology in 3.5 month-old corneas was observed compared to 3 month-old corneas prior to UMSC administration (Fig. 1C and Fig. 2E and F). Significant improvement was observed in 5 of the 6 corneas from mice treated at 3 months of age. UMSC transplantation therefore not only successfully impeded the progression but also improved the corneal manifestations (corneal haze) of MPS VII mice. Moreover, MPS VII treated with UMSC presented a decrease in corneal thickness ranging from 2 to 8 μm when compared to the contralateral untreated cornea (Figure 1).

Collagen disposition in corneas

In order to investigate whether the decrease in corneal haze relates to an overall improvement in collagen matrix disposition in treated corneas, we evaluated the collagen

network using second harmonic generation (SHG). SHG did not reveal a significant alteration in collagen fiber organization through forward scatter; however, the backscatter images demonstrated regional corneal haze in the untreated MPS VII corneas. Backscatter analysis of MPS VII corneas revealed areas with subtle corneal haze and areas with severe corneal haze, however, corneas of MPS VII mice treated with UMSC presented a similar backscatter profile to the littermate controls further confirming the *in vivo* confocal microscopy results, as seen in a representative image of MPS VII mice treated with UMSC at 2 months (Fig. S4). This suggests that improved corneal haze is not directly caused by a rearrangement of collagen matrix.

Phalloidin and ZO-1 staining of Whole-mount corneas

Corneas excised from the eyeballs were stained with phalloidin and ZO-1 in order to further analyze the integrity of stromal keratocytes and corneal endothelium. Phalloidin staining revealed significantly improved keratocyte morphology in treated corneas compared to the untreated corneas confirming morphological changes of stromal keratocytes observed by *in vivo* HRT-II confocal microscopy (Fig. 3A). Untreated corneas displayed strong phalloidin staining revealing small rounded keratocytes as well as keratocytes with an amoeboid shape (Fig. 3A). Animals treated at 1, 2 and 3 months of age presented many dendritic shaped cells throughout the stroma composed of both transplanted DiI positive UMSC and DiI negative host stromal dendritic cells, host keratocytes which appeared to be amoeboid in the absence of UMSC treatment (Fig. 3B). Interestingly, phalloidin and ZO-1 staining of untreated corneas at 3.5 months of age revealed a loss of the hexagonal shape of the endothelial cells as well as both an increased size and irregular shape (Fig. 3A and Fig. S5). However, corneas from MPS VII treated at 1, 2 and 3 months of age presented endothelial integrity (Fig. 3A and Fig. S5). Therefore, UMSC transplantation impeded deterioration of both the corneal keratocytes and endothelial cells.

The presence of DiI positive UMSC could be observed throughout the stroma of all treated corneas (OD); e.g., Fig. 3B illustrates an MPS VII mouse treated at 3 months of age. Transplanted UMSC assumed a dendritic cell shape and established cell-cell communications with host keratocytes (Fig. 3B), which further elucidates the successful transplantation, survival and differentiation of UMSC in the host corneas. UMSC transplanted into 3 month-old mice and analyzed at 3.5 months of age present strong DiI staining. Interestingly, cells adjacent to the DiI positive cells present DiI positive vesicles in their cytoplasm, however, no DiI staining in the cell membrane. Thus, we hypothesize that intercellular trafficking of subcellular organelles between donor and recipient cells may take place providing a mechanism to explain how the intrastromal transplantation of UMSC in 3 month-old MPS VII improves keratocyte amoeboid morphology within 2 weeks of treatment.

GAG content in treated and untreated corneal stroma

In order to elucidate whether the transplanted UMSC are aiding in GAG turnover and reducing overall GAG content, both in the corneal stroma and keratocytes, immunohistochemistry was performed with anti-CS and anti-HS antibodies. Corneas from 3.5 month-old MPS VII presented a significant increase in both CS and HS accumulation, in both the corneal stroma and keratocytes, compared to littermate controls. In order to capture images of the littermate control and treated MPS VII mouse corneas, without overexposing MPS VII untreated corneas, faint staining is observed for the littermate control and treated MPS VII corneas (OD) (Fig. 4A). The distribution of CS and HS staining in the untreated MPS VII (OS) corneas reveals strong staining along the corneal lamellae, dense staining within the keratocytes and staining evidencing accumulation in clumps throughout the interfibrillar space. A drastic decrease in CS and HS staining was observed in the MPS VII corneas that received UMSC treatment. Thus, UMSC are actively aiding in recycling the

GAGs preventing exacerbated accumulation in the tissue. These results were further confirmed by Alcian blue staining where strong staining is observed solely in the untreated MPS VII corneas (OS) throughout the cornea, primarily in the posterior stroma (Fig. S6).

To further investigate the efficacy of the transplanted UMSC, the overall GAG content was quantified using the DMB assay. Each treated cornea (OD) presented a significant decrease of at least 20% in overall GAG content when compared to the contralateral untreated cornea (OS) (Figure 4B). Figure 4C demonstrates the average GAG content for OS, OD and littermate wild-type control corneas. A mean 30% decrease in GAG content was observed in treated corneas when compared to the untreated corneas. Moreover, the level of GAGs in the animals treated at 1 and 2 months (black circle and triangle, respectively) decreased to the level of the littermate controls (white circle), whereas the level of GAGs in the animals treated at 3 months (square) decreased significantly compared to the untreated corneas (Figure 4C).

Keratocyte lysosomal content after UMSC

Due to the improved stromal morphology in corneas treated at 3 months and the drastic decrease in GAG content both in keratocytes and throughout the stroma we investigated whether UMSC treatment leads to a decrease in lysosome content in host keratocytes. Corneas from 3.5 month-old untreated MPS VII presented a significant increase in the number and size of lysosomes which can be observed through LAMP2 staining (Fig. 4D). Moreover, the keratocytes in the MPS VII untreated corneas with a small rounded cell shape presented a cytoplasm with densely distributed enlarged lysosomes. LAMP2 staining revealed a significant decrease in the number and size of lysosomes throughout treated corneas compared to the untreated corneas, presenting lysosomal content comparable to that of littermate controls (Fig. 4D). Thus, the decrease in the number and size of lysosomes, even in corneas treated at 3 months of age, further suggests cell-cell trafficking of vesicles from the UMSC to the resident host cells enabling such host cells to metabolize GAGs which had accumulated in lysosomes during the 3 months prior to treatment.

Cell-cell trafficking between UMSC and host keratocytes

In order to determine whether cell-cell trafficking of lysosomal material could occur between the UMSC and host cells, UMSC were labeled with FM 1-43FX and administered to the corneas of 3 month-old MPS VII mice, and FM 1-43FX positive vesicles were analyzed after three days. UMSC can be observed within the stroma presenting dense FM 1-43FX positive vesicles throughout the cytoplasm. Interestingly, FM 1-43FX positive vesicles can also be observed in keratocytes throughout the entire stroma and in endothelial cells. Thus, the UMSC are communicating with host cells through cell-cell trafficking of small vesicles, namely exosomes (Fig. 5A).

Cell-cell trafficking from UMSC to fibroblasts

Co-cultures of MPS VII skin fibroblasts with UMSC previously labeled with LysoSensor™ Yellow/Blue DND-160 were performed in order to study the dynamics of the intercellular trafficking between live MPS VII cells and UMSC. LysoSensor is a probe used to measure the pH of subcellular organelles, such as lysosomes, in living cells which fluoresces blue in neutral environments and yellow/green in more acidic environments. UMSC presented both acidic and neutral organelles throughout the cytoplasm (Fig. 5B). When co-cultured with UMSC after 15 minutes, fibroblasts presented neutral organelles in the medium surrounding the cells (Fig. 5B). After 30 minutes the fibroblasts presented both acidic and neutral organelles within the cytoplasm (Fig. 5B). After 1 hour of co-culture with UMSC the MPS VII skin fibroblasts presented a vast majority of acidic organelles throughout the cytoplasm (Fig. 5B). Fibroblasts which were not co-cultured with UMSC presented no labeled

organelles. Thus, fibroblasts received neutral organelles from the UMSC through the culture medium, which were up-taken by the fibroblasts and fused with the lysosomes.

In order to determine whether the fibroblasts could successfully turnover the lysosomal accumulated material, the fibroblasts exposed to UMSC for 6 hours were stained with LAMP2. After 6 hours of co-culture, a significant decrease in number and size of lysosomes was evidenced (Fig. 5C and D). Therefore, the fibroblasts were able to successfully turnover of the accumulated GAGs reducing the overall number and size of lysosomes potentially by receiving active β -glucuronidase from the UMSC.

Discussion

MPS are chronic and progressive diseases which evolve to multisystem deterioration and, in more severe cases, death within the first decade of life. To date, treatments involve enzyme replacement therapy and/or allogeneic haematopoietic stem cell transplantation which delay the progression of the symptoms and prolong survival^{14–16, 20}. However, these treatments are not effective for improving corneal clouding, skeletal disorders (due to the reduced vascularity of these tissues) and impaired mental development (due the blood brain barrier)^{21–24, 33}. Therefore, corneal clouding is ultimately treated by corneal transplantation (keratoplasty) which requires general anesthetic; however, MPS patients also suffer respiratory dysfunction and/or severe cardiomyopathy so, in many cases, they are too frail to undergo surgery. Moreover, availability of transplantable corneas is also a limiting factor for treating corneal clouding and ultimately visual impairment associated with MPS. Therefore, we suggest UMSC transplantation as an alternative treatment in lieu of keratoplasty for MPS patients.

UMSC transplanted into the corneas of 1, 2 and 3 month-old MPS VII mice survived host rejection and assumed a keratocyte phenotype, which was previously shown by our group for treating *Lum*^{-/-} mice^{26, 34}. MPS are progressive diseases involving the accumulation of products of incomplete GAG digestion which ultimately leads to cell death. With cell death the GAG products are expelled into the ECM which further enhances the progression of the disease. Therefore, UMSC which attain the ability to differentiate and become resident stromal cells may substitute lost host keratocyte function. Moreover, the presence of UMSC in the corneal stroma, which are capable of taking up and recycling GAGs and the GAG degradation products, impedes further progression of the disease. The improvement of the corneas transplanted with UMSC was evident through *in vivo* confocal microscopy. MPS VII corneas transplanted with UMSC at 1 and 2 months of age presented drastically reduced corneal haze and keratocytes with a dendritic cell shape when analyzed at 3.5 months of age, while untreated mice presented significant corneal haze and keratocytes with an amoeboid cell shape throughout the stroma at this same timeframe. Therefore, UMSC when administered to MPS VII at 1 and 2 months of age were able to impede the progression of the disease to an extent that stromal and keratocyte morphology were similar to that of littermate control mice. Moreover, MPS VII is a rare disorder which very often is diagnosed after the disease has significantly progressed and the patients already display certain symptoms. In order to evaluate the efficiency of treatment with UMSC for onset symptoms, MPS VII mice were treated at 3 months of age and analyzed at 3.5 months of age. A significant improvement was observed for MPS VII corneas treated with UMSC compared to untreated controls. The corneas of MPS VII mice treated with UMSC at 3 months of age presented a significant decrease in keratocytes with an amoeboid cell shape, preserved endothelial morphology and a significant decrease in corneal haze. Therefore, the treatment of MPS VII mice with onset of pathological corneal symptoms improved overall stromal morphology 2 weeks after transplantation, and, therefore, UMSC transplantation could be potentially used to treat MPS patients in lieu of keratoplasty.

Analysis of MPS VII corneas treated at 3 months of age revealed a drastic decrease in overall GAG content as well as number and size of lysosomes in keratocytes suggesting that the UMSC were aiding the stromal host cells to metabolize GAG content accumulated throughout the 3 months prior to treatment. Based on the drastic improvement in keratocyte morphology in mice treated at 3 months of age, together with a decrease in GAG content and the number and size of lysosomes, we postulate that UMSC do more than solely turnover GAGs accumulated in the ECM. We hypothesize that the host keratocytes and endothelial cells could receive active α -glucuronidase from the UMSC thus enabling the cells to catabolize the accumulated GAGs from within the lysosomes. α -glucuronidase contains a mannose 6-phosphate (M6P) moiety on the carbohydrate chains which enables the directing of this enzyme to the lysosomes from both the Golgi apparatus and the ECM via binding to the insulin-like growth factor II/cation-independent mannose 6-phosphate receptor (IGF-II/MPR). We have previously shown that transplanted UMSC establish cell-cell communications with stromal host cells²⁶. Thus, we hypothesize that intercellular trafficking of active α -glucuronidase could occur between these two cell types. In this scenario, host keratocytes could receive active α -glucuronidase from transplanted UMSC by established cell-cell communications, by enzyme secretion and/or by intercellular trafficking of vesicles directing active α -glucuronidase to host lysosomes, enabling continuation of the sequential degradation. Recently, mesenchymal stem cells (MSC) have been shown to communicate with host cells through exosomes, small endosome-derived lipid nanoparticles (50–120 nm) actively secreted by exocytosis, which play an important role in intercellular trafficking. Exosomes are constitutively released by most cells; however, their content may be regulated upon induction in pathological conditions. Increasing evidence suggests that the therapeutic efficacy of MSC therapy is not solely due to differentiation into host cell types at the site of transplantation but also due to cell-cell communication through exosomes^{35–37}. The diversity in exosome content secreted by MSC has also been attributed to the therapeutic efficacy of these cells in treating a plethora of diseases such as ischemia and MPS I with bone fractures³⁸. Moreover, MSC exosomes have been shown to contain a vast array of proteolytic enzymes and glycosidases³⁹. The finding that MSC exosomes contain glycosidases such as α -L-fucosidase, which hydrolyses the O- and S-glycosyl compound which, when deficient, leads to the lysosomal storage disease fucosidosis, further suggests that these diseases can be treated with certain exosome populations³⁹. When UMSC labeled with FM 1–43, a lipophilic dye used to study cell vesiculation, were administered to the MPS VII stroma and analyzed after 3 days a distribution of UMSC vesicles is clearly seen throughout the stroma and endothelium. Co-cultures of UMSC labeled with LysoSensorTM Yellow/Blue DND-160 and primary MPSVII skin fibroblasts revealed that the UMSC indeed secrete vesicles which are successfully up-taken by the fibroblasts and proceed to fuse with the lysosomes, supporting the notion that intercellular trafficking of vesicles between UMSC and host cells could deliver active α -glucuronidase, enabling the host cells to catabolize the accumulated GAGs.

Collectively, our data shows that human UMSC transplanted into MPS VII mouse corneas survived rejection and differentiated into resident stromal cells. The transplanted UMSC aid in the recycling of both the extracellular GAG content as well as accumulation within the keratocytes and, therefore, avoided the accumulation of GAGs in the corneal stroma and keratocytes (Fig. 6). MPS VII corneas treated with UMSC at an earlier time point, e.g., 1 and 2 months of age, displayed healthy keratocytes and no corneal clouding, which demonstrates that UMSC were able to impede the progression of the disease and the MPS VII mice corneas presented similar stromal morphology to littermate controls. Therefore, MPS VII patients would benefit greatly from early treatment with UMSC, possibly at the time of diagnosis, thereby preventing the development of corneal clouding and visual impairment. Moreover, UMSC were shown to communicate with host keratocytes through intercellular trafficking of vesicles, enabling the significant improvement observed when

MPS VII mice were treated with the onset of corneal symptoms, which suggests that UMSC can be used as an alternative treatment in lieu of corneal transplantation in advanced MPS VII patients. The cornea is affected in all MPS subtypes described to date, however, MPS I, MPS II, MPS VI and MPS VII, display significant corneal clouding due to the accumulation of GAGs within the cornea. Therefore, the success in treating corneal clouding associated with MPS VII could be transposed to other MPS as well as to other metabolic disorders. This data further supports that allograft of human UMSC into human corneas has great potential for being successful in treating human corneal congenital metabolic diseases.

Supplementary Material

Refer to Web version on PubMed Central for supplementary material.

Acknowledgments

The authors thank Dr. Tarsis F. Gesteira (Childrens Hospital, Cincinnati) for his valuable help throughout the study. This work was supported in part by grants NIH/NEI RO1 EY021768, Research to Prevent Blindness, Ohio Lions eye Research Foundation and Arthritis Research UK Grant 19858.

Abbreviations

UMSC	umbilical cord mesenchymal stem cells
MPS	Mucopolysaccharidosis
GAG	Glycosaminoglycan
PG	Proteoglycan
ECM	extracellular matrix
LAMP2	Lysosomal-associated membrane protein 2
OD	right eye
OS	left eye

References

1. Freeze HH. Genetic Disorders of Glycan Degradation. 2009
2. Cantz M, Gehler J. The mucopolysaccharidoses: inborn errors of glycosaminoglycan catabolism. *Hum Genet.* 1976; 32:233–255. [PubMed: 820626]
3. Bernsen PL, Wevers RA, Gabreels FJ, et al. Phenotypic expression in mucopolysaccharidosis VII. *J Neurol Neurosurg Psychiatry.* 1987; 50:699–703. [PubMed: 3112309]
4. Neufeld EF, d'Azzo A. Biosynthesis of normal and mutant beta-hexosaminidases. *Adv Genet.* 2001; 44:165–171. [PubMed: 11596981]
5. Tomatsu S, Montano AM, Dung VC, et al. Mutations and polymorphisms in GUSB gene in mucopolysaccharidosis VII (Sly Syndrome). *Hum Mutat.* 2009; 30:511–519. [PubMed: 19224584]
6. Gitzelmann R, Wiesmann UN, Spycher MA, et al. Unusually mild course of beta-glucuronidase deficiency in two brothers (mucopolysaccharidosis VII). *Helv Paediatr Acta.* 1978; 33:413–428. [PubMed: 101485]
7. Beaud AL, Roufa DJ, Caskey CT. Mutations affecting the structure of hypoxanthine: guanine phosphoribosyltransferase in cultured Chinese hamster cells. *Proc Natl Acad Sci U S A.* 1973; 70:320–324. [PubMed: 4119786]
8. Sly WS, Brot FE, Glaser J, et al. Beta-glucuronidase deficiency mucopolysaccharidosis. *Birth Defects Orig Artic Ser.* 1974; 10:239–245. [PubMed: 4282258]
9. Neufeld EF, Cantz MJ. Corrective factors for inborn errors of mucopolysaccharide metabolism. *Ann N Y Acad Sci.* 1971; 179:580–587. [PubMed: 4255108]

10. Vogler C, Birkenmeier EH, Sly WS, et al. A murine model of mucopolysaccharidosis VII. Gross and microscopic findings in beta-glucuronidase-deficient mice. *Am J Pathol.* 1990; 136:207–217. [PubMed: 2105058]
11. Sands MS, Vogler CA, Ohlemiller KK, et al. Biodistribution, kinetics, and efficacy of highly phosphorylated and non-phosphorylated beta-glucuronidase in the murine model of mucopolysaccharidosis VII. *J Biol Chem.* 2001; 276:43160–43165. [PubMed: 11562370]
12. Kenyon KR. Ocular manifestations and pathology of systemic mucopolysaccharidoses. *Birth Defects Orig Artic Ser.* 1976; 12:133–153. [PubMed: 821556]
13. Nelson J. Incidence of the mucopolysaccharidoses in Northern Ireland. *Hum Genet.* 1997; 101:355–358. [PubMed: 9439667]
14. Barton NW, Furbish FS, Murray GJ, et al. Therapeutic response to intravenous infusions of glucocerebrosidase in a patient with Gaucher disease. *Proc Natl Acad Sci U S A.* 1990; 87:1913–1916. [PubMed: 2308952]
15. Winkel LP, Van den Hout JM, Kamphoven JH, et al. Enzyme replacement therapy in late-onset Pompe's disease: a three-year follow-up. *Ann Neurol.* 2004; 55:495–502. [PubMed: 15048888]
16. Rohrbach M, Clarke JT. Treatment of lysosomal storage disorders : progress with enzyme replacement therapy. *Drugs.* 2007; 67:2697–2716. [PubMed: 18062719]
17. Clarke LA. The mucopolysaccharidoses: a success of molecular medicine. *Expert Rev Mol Med.* 2008; 10:e1. [PubMed: 18201392]
18. Beck M. Therapy for lysosomal storage disorders. *IUBMB Life.* 2010; 62:33–40. [PubMed: 20014233]
19. Papadia F, Lozupone MS, Gaeta A, et al. Long-term enzyme replacement therapy in a severe case of mucopolysaccharidosis type II (Hunter syndrome). *Eur Rev Med Pharmacol Sci.* 2011; 15:253–258. [PubMed: 21528770]
20. Lachmann R. Treatments for lysosomal storage disorders. *Biochem Soc Trans.* 2010; 38:1465–1468. [PubMed: 21118108]
21. Vogler C, Sands MS, Levy B, et al. Enzyme replacement with recombinant beta-glucuronidase in murine mucopolysaccharidosis type VII: impact of therapy during the first six weeks of life on subsequent lysosomal storage, growth, and survival. *Pediatr Res.* 1996; 39:1050–1054. [PubMed: 8725268]
22. Vogler C, Sands MS, Galvin N, et al. Murine mucopolysaccharidosis type VII: the impact of therapies on the clinical course and pathology in a murine model of lysosomal storage disease. *J Inherit Metab Dis.* 1998; 21:575–586. [PubMed: 9728337]
23. Sands MS, Vogler C, Kyle JW, et al. Enzyme replacement therapy for murine mucopolysaccharidosis type VII. *J Clin Invest.* 1994; 93:2324–2331. [PubMed: 8200966]
24. Tomatsu S, Montano AM, Ohashi A, et al. Enzyme replacement therapy in a murine model of Morquio A syndrome. *Hum Mol Genet.* 2008; 17:815–824. [PubMed: 18056156]
25. Al Sawaf S, Mayatepek E, Hoffmann B. Neurological findings in Hunter disease: pathology and possible therapeutic effects reviewed. *J Inherit Metab Dis.* 2008; 31:473–480. [PubMed: 18618289]
26. Liu H, Zhang J, Liu CY, et al. Cell therapy of congenital corneal diseases with umbilical mesenchymal stem cells: lumican null mice. *PLoS One.* 2010; 5:e10707. [PubMed: 20502663]
27. Kao WW, Liu CY. Roles of lumican and keratocan on corneal transparency. *Glycoconjugate journal.* 2002; 19:275–285. [PubMed: 12975606]
28. Carlson EC, Liu CY, Chikama T, et al. Keratocan, a cornea-specific keratan sulfate proteoglycan, is regulated by lumican. *J Biol Chem.* 2005; 280:25541–25547. [PubMed: 15849191]
29. Kadler KE, Hill A, Canty-Laird EG. Collagen fibrillogenesis: fibronectin, integrins, and minor collagens as organizers and nucleators. *Current opinion in cell biology.* 2008; 20:495–501. [PubMed: 18640274]
30. Chen LD, Hazlett LD. Perlecan in the basement membrane of corneal epithelium serves as a site for P. aeruginosa binding. *Current eye research.* 2000; 20:260–267. [PubMed: 10806439]
31. Stepp MA, Gibson HE, Gala PH, et al. Defects in keratinocyte activation during wound healing in the syndecan-1-deficient mouse. *Journal of cell science.* 2002; 115:4517–4531. [PubMed: 12414997]

32. Alonso-Fernandez JR, Fidalgo J, Colon C. Neonatal screening for mucopolysaccharidoses by determination of glycosaminoglycans in the eluate of urine-impregnated paper: preliminary results of an improved DMB-based procedure. *Journal of clinical laboratory analysis*. 2010; 24:149–153. [PubMed: 20486194]
33. Rowan DJ, Tomatsu S, Grubb JH, et al. Long circulating enzyme replacement therapy rescues bone pathology in mucopolysaccharidosis VII murine model. *Mol Genet Metab*. 2012; 107:161–172. [PubMed: 22902520]
34. Liu H, Zhang J, Liu C'Y, et al. Bone marrow mesenchymal stem cells can differentiate and assume corneal keratocyte phenotype. *J Cell Mol Med*. 2012; 16:1114–1124. [PubMed: 21883890]
35. Iso Y, Spees JL, Serrano C, et al. Multipotent human stromal cells improve cardiac function after myocardial infarction in mice without long-term engraftment. *Biochem Biophys Res Commun*. 2007; 354:700–706. [PubMed: 17257581]
36. Noiseux N, Gnecci M, Lopez-Ilasaca M, et al. Mesenchymal stem cells overexpressing Akt dramatically repair infarcted myocardium and improve cardiac function despite infrequent cellular fusion or differentiation. *Mol Ther*. 2006; 14:840–850. [PubMed: 16965940]
37. da Silva Meirelles L, Caplan AI, Nardi NB. In search of the in vivo identity of mesenchymal stem cells. *Stem Cells*. 2008; 26:2287–2299. [PubMed: 18566331]
38. Giordano A, Galderisi U, Marino IR. From the laboratory bench to the patient's bedside: an update on clinical trials with mesenchymal stem cells. *J Cell Physiol*. 2007; 211:27–35. [PubMed: 17226788]
39. Lai RC, Tan SS, Teh BJ, et al. Proteolytic Potential of the MSC Exosome Proteome: Implications for an Exosome-Mediated Delivery of Therapeutic Proteasome. *Int J Proteomics*. 2012; 2012:971907. [PubMed: 22852084]

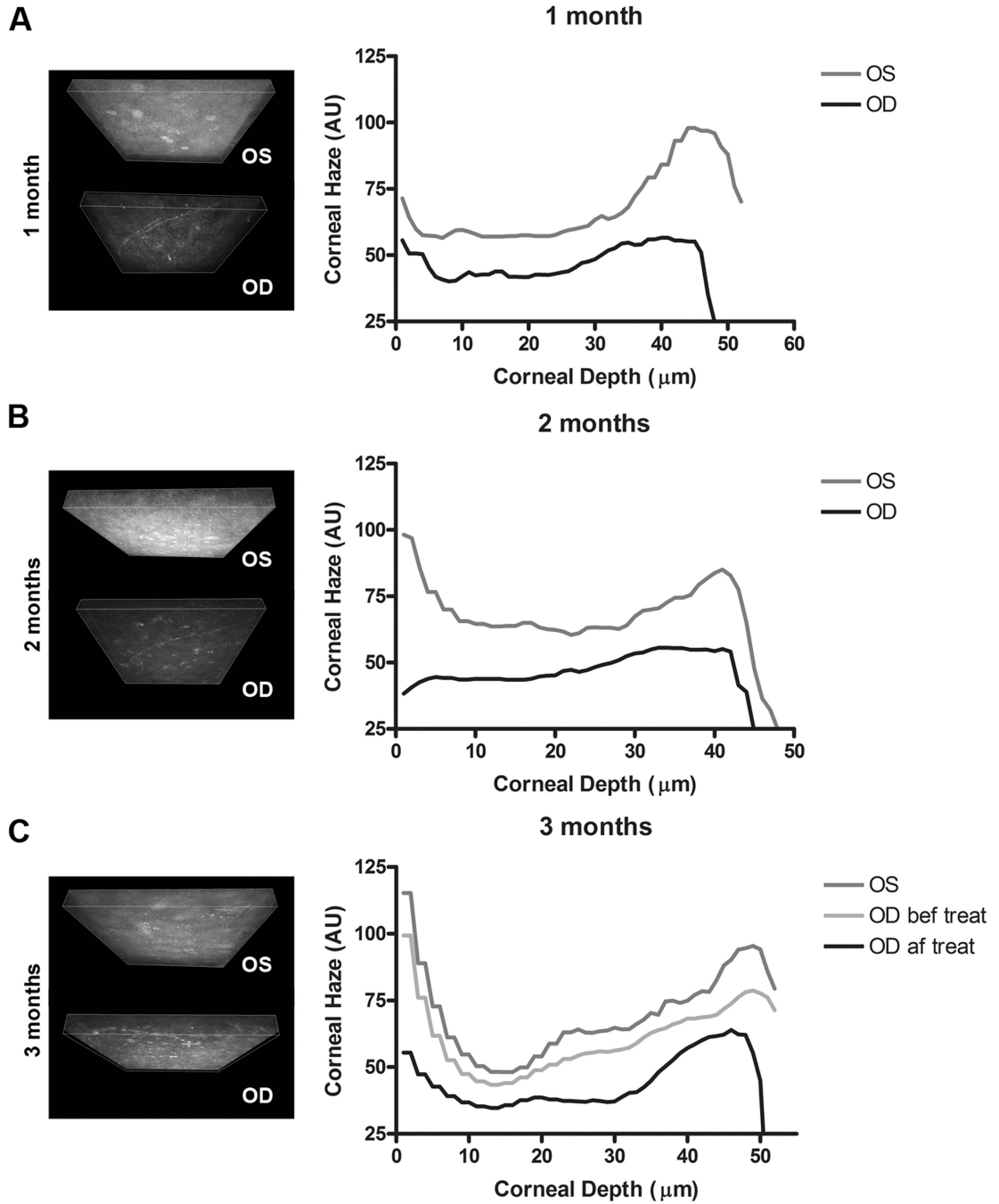


Figure 1. Corneal haze by In vivo confocal microscopy. Analysis of stromal haze was performed using Heidelberg Retinal Tomograph-HRTII Rostock Cornea Module (HRT-II, Heidelberg Engineering Inc., Germany). A series of images was collected to cover the whole stromal thickness as a continuous z-axis scan through the entire corneal stroma at 2 μm increments starting from the basal layer of the corneal epithelium and ending at the corneal endothelium. 3D reconstitution and histograms of light scattering were performed of images captured from (A) animals treated at 1 month, (B) animals treated at 2 months, and (C) animals treated at 3 months. Histograms produced using Fiji reveal significant corneal haze in untreated MPS VII corneas (OS) at 3.5 months (black graphs) and in the stroma of mice

treated at 3 months prior to UMSC administration (C before treat). A significant decrease in haze can be observed in treated corneas at all time frames (OD) (grey graph).

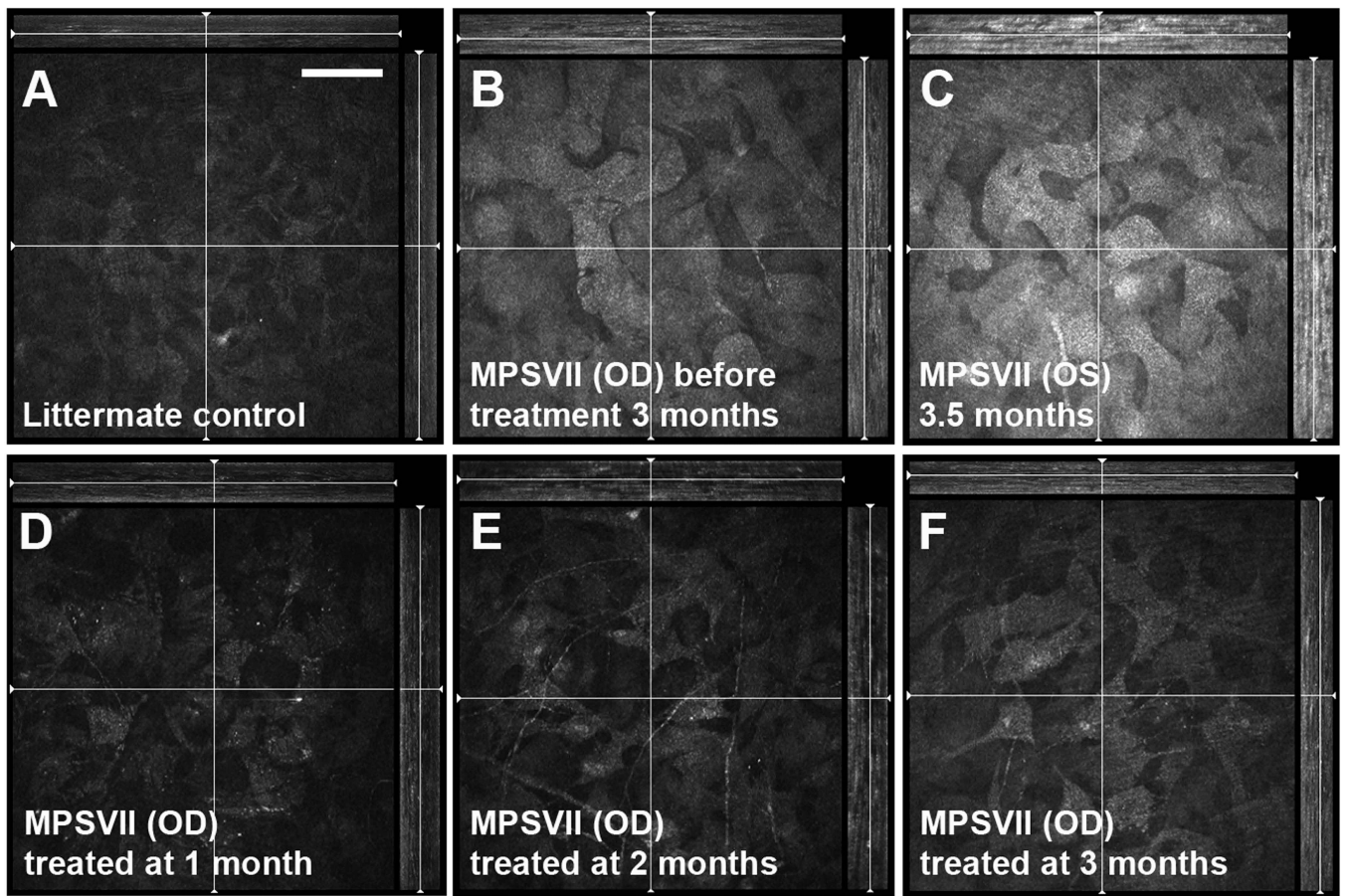


Figure 2.

Corneal morphology by in vivo confocal microscopy. Analysis of stromal morphology was performed using in vivo confocal microscopy. A representative image at the stromal depth of approximately 8 μm is shown for (A) littermate control wild-type mouse; (B) untreated MPSVII mice at 3 months; (C) untreated MPSVII mice at 3.5 months; (D) animals treated at 1 month at the conclusion of treatment; (E) animals treated at 2 months at the conclusion of treatment; (F) animals treated at 3 months at the conclusion of treatment. Amoeboid keratocytes are present throughout the stroma of untreated MPS VII corneas, however, a significant decrease in amoeboid keratocytes is observed in the stroma of mice treated at all time frames. Scale bar 50 μm .

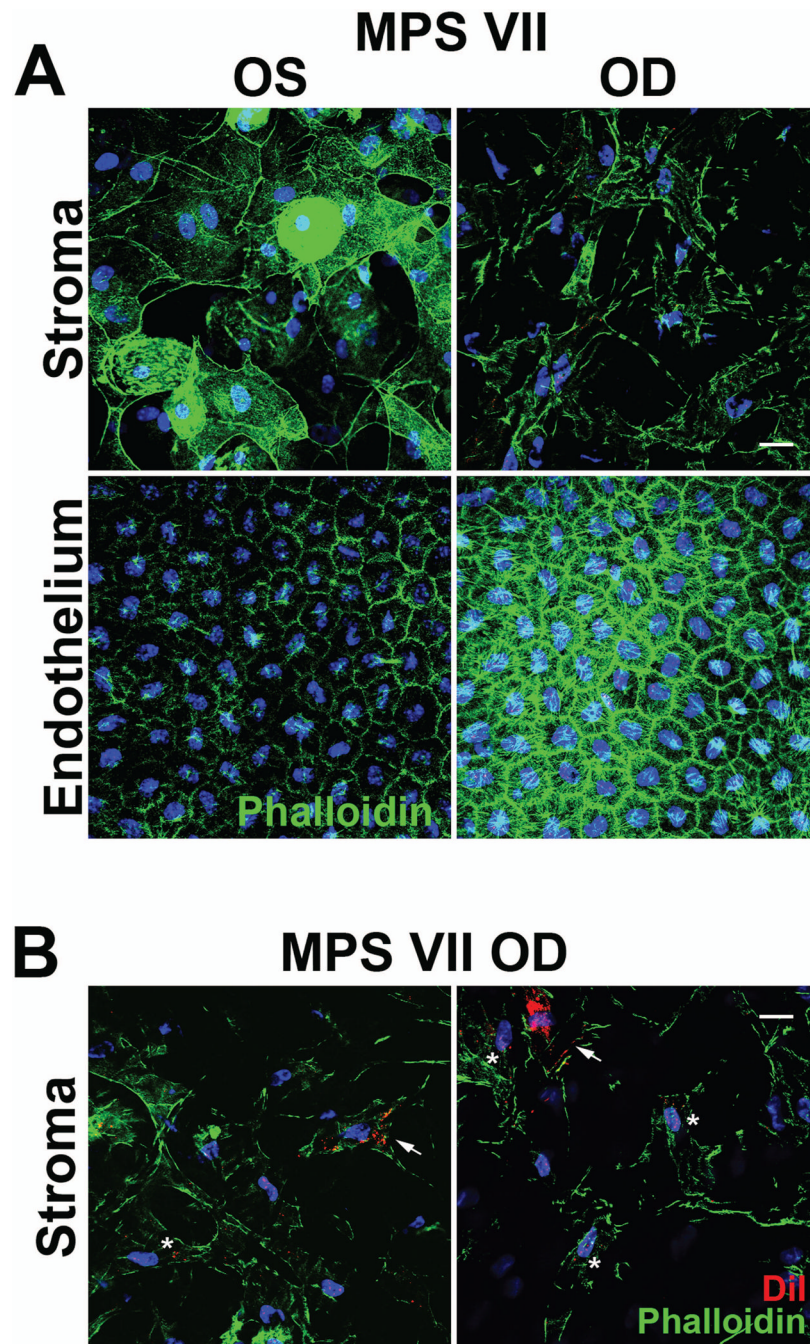


Figure 3. Phalloidin staining after UMSC treatment. Corneas excised from the eyeballs were stained with phalloidin (green) in order to analyze the integrity of stromal keratocytes and endothelium (A and B). Phalloidin staining revealed significantly improved keratocyte morphology in treated corneas compared to the untreated corneas. (A) Untreated corneas (OS) display strong phalloidin staining revealing small rounded keratocytes as well as keratocytes with an amoeboid shape while treated corneas (OD) present dendritic host keratocytes. (B) DiI labeled UMSC (red) were present throughout the stroma of treated corneas. DiI positive cells (arrow) can be observed in the stroma establishing cell-cell

contacts with host keratocytes (Asterisk). DiI speckles can be observed in host keratocytes surrounding DiI positive UMSC. Scale bar 20 μm .

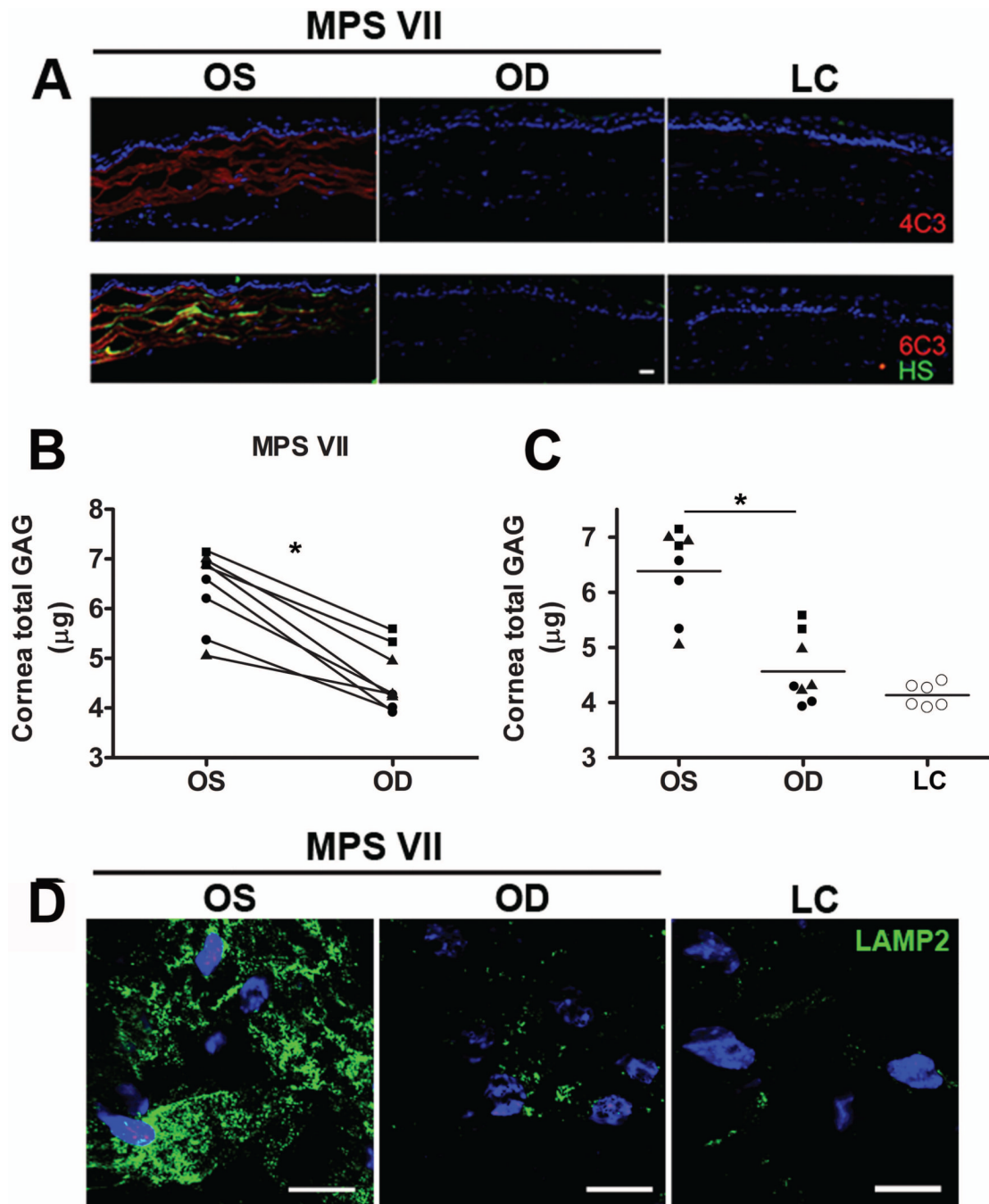


Figure 4.

Effectiveness of stem cell treatment by analysis of glycosaminoglycan and lysosomal content in MPS VII corneas treated with UMSC. (A) Immunocytochemistry was performed with mouse monoclonal anti-CS native sulfation motif (clones 4C3 and 6C3) and anti-HS (10E4 epitope). Corneas from 3.5 month-old MPS VII (OS) present a significant increase in both CS (red) and HS (green) accumulation with strong staining along the corneal lamellae, dense staining within the keratocytes and staining evidencing accumulation in clumps throughout the interfibrillar space. A drastic decrease in CS and HS staining was observed in the MPS VII corneas that received UMSC treatment (OD). (B and C) The total GAG content was measured using DMB. (B) Treated corneas (OD) at 1 month (black circle), 2 months

(triangle) and 3 months (square) presented a significant reduction of at least 20% in overall GAG content when compared to the contralateral untreated corneas (OS). (C) A mean 30% reduction in GAG content was observed in treated corneas (OD) when compared to the untreated corneas (OS). The level of GAGs in the animals treated at 1 and 2 months (black circle and triangle, respectively) decreased to the level of the littermate wild-type controls (white circle), whereas the level of GAGs in the animals treated at 3 months (square) decreased significantly compared to the untreated corneas. (D) An overall decrease in lysosomal content (green) was observed in keratocytes throughout the stroma of animals treated at all-time points. A representative image at an approximate stromal depth of 10 μm is shown for LAMP2 staining in host keratocytes of animals treated at 2 months demonstrates the drastic decrease in the number and size of lysosomes in DiI negative cells. Nuclei were stained with DAPI (blue). Scale bar 20 μm . * $p < 0.05$.

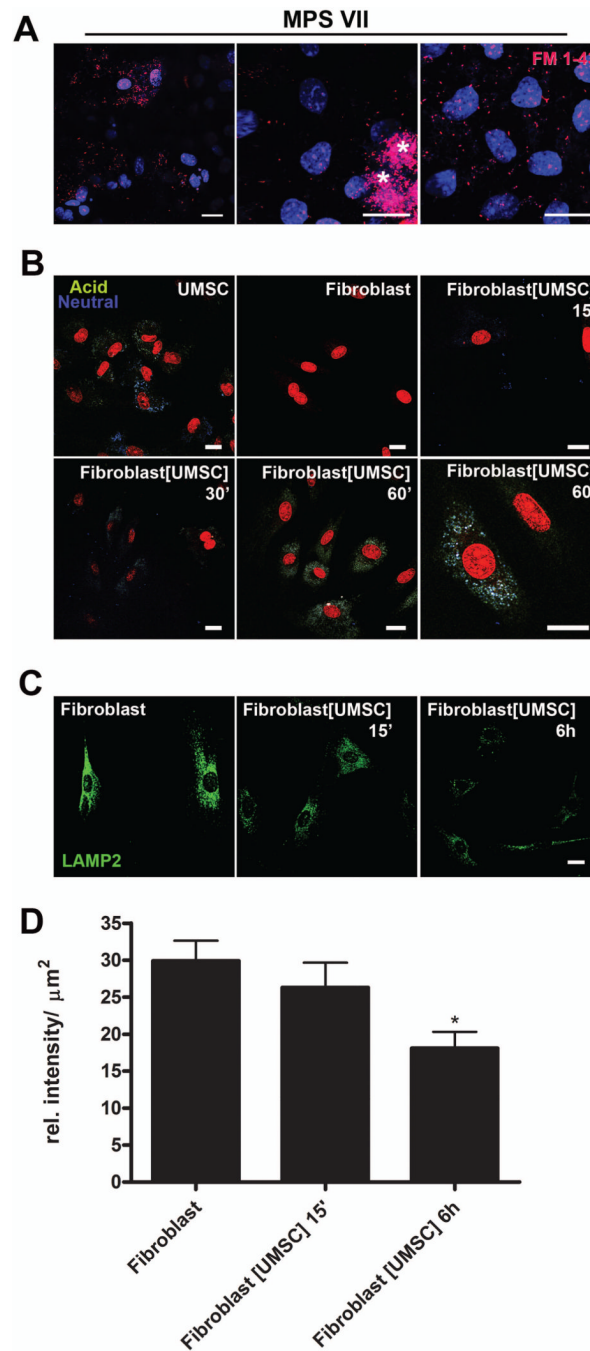


Figure 5.

Lysosomal content and cell-cell trafficking between UMSC and MPS VII keratocytes and fibroblasts. (A) UMSC (asterisk) were labeled with FM 1-43FX (red) prior to intrastromal administration and eyeballs were excised after 3 days and corneas processed for whole mount. (B) MPS VII skin fibroblasts exposed to UMSC that had been previously labeled with LysoSensor™ Yellow/Blue DND-160 and seeded in transwell inserts with 0.44 μm pores for 15, 30 and 60 minutes. The live cells were analyzed using a Zeiss LSM710 confocal microscope. The nuclei of the UMSC and fibroblasts were labeled with SYTO® 59 (red). Neutral organelles are observed as blue and acid organelles as yellow/green. Scale bar 20 μm . (C) MPS VII fibroblasts placed in co-culture with UMSC for 15 minutes or 6 hours

and labeled with LAMP2 (green) in order to evaluate the lysosomal content. Naïve fibroblasts were used as the control. Nuclei were stained with DAPI (blue). Scale bar 20 μm . (D) The average number of pixels in 12 images for each experimental condition was calculated and the results displayed in a bar graph evidencing a statistically significant decrease in lysosome content in MPS VII fibroblasts exposed to UMSC. * $p < 0.05$.

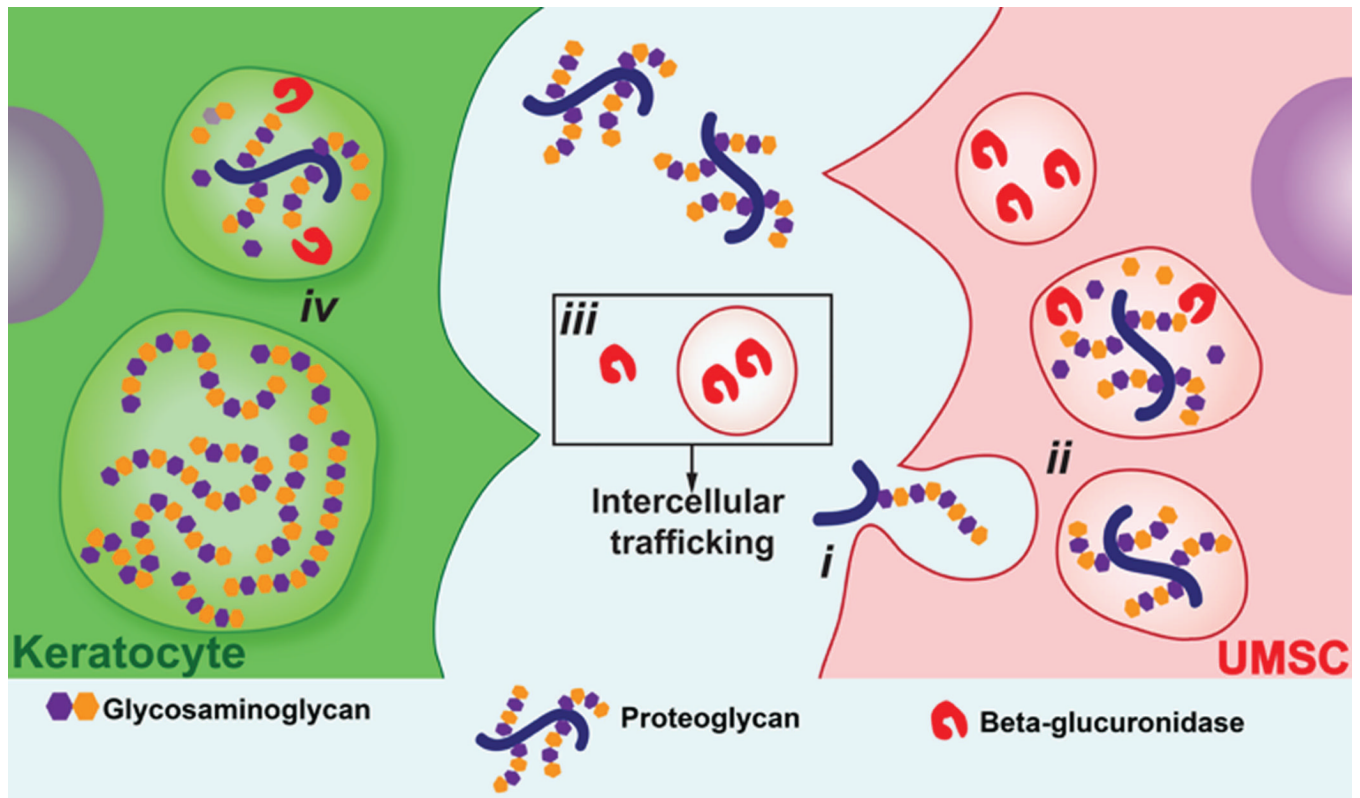


Figure 6.

A schematic representation of the mechanism by which UMSC (red) aid corneal GAG turnover in MPSVII mice. (i) Endocytosis of accumulated extracellular GAGs and PGs by UMSC; (ii) UMSC catabolize the GAGs; (iii) intercellular trafficking active β -glucuronidase between UMSC and host keratocytes; (iv) sequential degradation of accumulated GAGs in host keratocyte.